Material properties and membrane residual stresses of S690 high strength steel welded I-sections after exposure to elevated temperatures

Andi Su [a], Yao Sun [a], Yating Liang [b], Ou Zhao [*a]

[a] School of Civil and Environmental Engineering, Nanyang Technological University, Singapore

[b] School of Engineering, University of Glasgow, Glasgow, UK

[*] Corresponding author, Email: ou.zhao@ntu.edu.sg

Abstract

This paper reports a thorough experimental investigation into the material properties and membrane residual stresses of S690 high strength steel welded I-sections after exposure to seven levels of elevated temperatures ranging from 30 ºC (room temperature) to 950 ºC. The experimental programme included heating, soaking and cooling of S690 high strength steel coupons and welded I-section specimens as well as post-fire material tensile coupon tests and membrane residual stress measurements, with the experimental rigs, procedures and results fully reported. The key post-fire material properties were then carefully analysed together with the test data collected from the existing literature, and a new set of retention factor curves of simple multi-linear shapes was proposed and shown to result in accurate predictions of post-fire yield and ultimate stresses for S690 high strength steel after exposed to elevated temperatures. Regarding post-fire membrane residual stresses, the measured distribution pattern and peak amplitudes in S690 high strength steel welded I-section after exposed to an elevated temperature of 300 ºC generally remained unchanged in comparison with those in S690 high strength steel welded I-section at room temperature. However, for higher elevated temperatures ranging from 600 ºC to 950 ºC, the peak values of both compressive and tensile membrane residual stresses dramatically decreased, and moreover the discrepancy between the peak compressive and tensile membrane residual stress values became smaller and the transition regions (where the peak tensile residual stresses are changed to the peak compressive residual stresses) became narrower; this can be attributed to the fact that prominent elastic strain redistribution and residual stress relaxation of steel starts from around 500 ºC–600 ºC. A membrane residual stress predictive model was proposed for S690 high strength steel welded I-sections after exposed to elevated temperatures, and shown to well represent the measured membrane residual stress patterns and amplitudes over the full temperature range from 30 ºC to 950 ºC.

Keywords: Heating, soaking and cooling processes; High strength steel grade S690; Post-fire material properties; Post-fire membrane residual stresses; Predictive models; Residual stress measurements; Retention factors; Tensile coupon tests; Welded I-section.

1. Introduction

High strength steels are being increasingly utilised in civil engineering applications, especially for long-span bridges and high-rise buildings, owing to the high strength-to-weight ratios [1,2]. Given that most of the existing design standards for high strength steel structures were established through directly mirroring the provisions and formulations given in the corresponding normal strength mild steel design standards, experimental and numerical studies have been prompted, with the aim of verifying the behaviour and capacities of different types of high strength steel structural components with various cross-section shapes and devising more improved and efficient design methods for them. With regard to S690 high strength steel welded I-sections, Sun et al. [3] measured the membrane residual stresses in four S690 high strength steel welded I-sections, verified their patterns and amplitudes, and finally proposed a predictive model. Sun et al. [3] and Rasmussen and Hancock [4] performed concentric compression tests on S690 high strength steel welded I-section stub columns, quantified their cross-section compressive resistances and evaluated the accuracy of the relevant codified design rules on slenderness limits and effective element widths. The flexural behaviour and strengths of S690 high strength steel welded I-section beams bent about both the major and minor principal axes were experimentally and numerically examined by Wang [5] and Sun et al. [6], with the codified slenderness limits and design flexural strengths assessed. A series of experimental and numerical studies on S690 high strength steel welded I-section columns [7–9] and beam-columns [10] were performed to respectively investigate their member stability in pure compression and combined compression and bending moment, and on the basis of the experimental and numerical results, the relevant design provisions prescribed in the existing design standards were examined, followed by the development of new design proposals. It is worth noting that the aforementioned studies were conducted on S690 high strength steel welded I-section structural components at room temperature; however, research into their behaviour under fire and post-fire conditions remains scarce, despite three experimental studies

[11–13] on the post-fire material properties of S690 high strength steel. This prompts a research project being carried out at Nanyang Technological University, with the aim of examining the material and structural behaviour of S690 high strength steel welded I-section members in fire and after exposure to fire.

The present study focuses on the post-fire material properties and membrane residual stresses of S690 high strength steel welded I-sections, underpinned by a thorough testing programme. Seven pairs of (longitudinal and transverse) coupons and welded I-section specimens were firstly heated to seven levels of elevated temperatures ranging from 30 ºC (i.e. room temperature) to 950 ºC and then naturally cooled down; this was followed by post-fire tensile coupon tests and membrane residual stress measurements. The derived material stress–strain curves of the S690 high strength steel longitudinal and transverse coupons after exposed to elevated temperatures were discussed, with the degree of anisotropy investigated. The obtained key post-fire material properties, together with those reported in previous experimental studies [11–13], were carefully studied, and then employed to develop simple but precise retention factors for material modulus and strengths. The patterns and amplitudes of the measured membrane residual stresses in S690 high strength steel welded I-sections after exposure to elevated temperatures were thoroughly analysed, with a predictive model proposed.

2. Testing programme

2.1. General

A thorough testing programme was firstly conducted to establish a data bank on residual material properties and membrane residual stresses of S690 high strength steel welded I-sections after exposure to elevated temperatures. In the present testing programme, a total of seven levels of temperatures T, including 30 ºC (i.e. room temperature) and 300 ºC, 600 ºC, 700 ºC, 800 ºC, 900 ºC and 950 ºC (i.e. elevated temperatures), were considered, and accordingly seven nominally identical S690 high strength steel welded I-section I-100×100×5 specimens were prepared for membrane residual stress measurements; note that the cross-section identifier is consisted of a letter 'I' signifying an I-shaped section and the nominal cross-section sizes in millimetre, i.e. outer section depth h × flange width b_f × wall thickness t – see Fig. 1. All the seven S690 high strength steel welded I-section I-100×100×5 specimens were fabricated from the same batch of 5 mm thick S700MC high strength steel sheets by robotic gas metal arc welding, ensuring that membrane residual stresses with the same pattern and amplitudes were introduced into the specimens after welding at room temperature. The detailed welding process is described as follows. Three 5 mm thick plates were carefully positioned on the flat work bench to form a well-aligned I-shaped profile. Two robotic arms were then located at the same side of the top and bottom web-to-flange junctions at one end of the I-section profile, and two more robotic arms were placed anti-symmetrically to their counterparts at the other end of the I-section profile. The four robotic arms started welding at the same time from different sides of the web-to-flange junctions at different ends; this welding strategy helped minimise the cross-section and member distortion during welding. A total of fourteen coupons were cut from the S700MC high strength steel virgin sheets, with seven extracted along the sheet rolling direction (termed longitudinal coupons) and another seven cut perpendicular to the sheet rolling direction (termed transverse coupons), and the geometric sizes of the coupons were in line with the specific requirements set out in EN ISO 6892-1 [14], with the gauge length equal to 50 mm and parallel width of 12 mm. For each considered temperature level, two coupons (including one longitudinal coupon and one transverse coupon) and one welded I-section specimen were heated, soaked and cooled together under the same condition of environment, ensuring that both the coupons and welded I-section specimen followed the same heating, soaking and cooling processes.

2.2. Heating, soaking and cooling of coupons and welded I-section specimens

A Nabertherm forced convection chamber furnace was utilised to heat the S690 high strength steel welded I-section specimens and longitudinal and transverse coupons. Fig. 2 depicts the chamber of the furnace, which contains a series of embedded heating elements distributed uniformly over the four sides of the chamber and is equipped with a fan and air baffles to allow for air circulation during heating, thus leading to a high degree of temperature uniformity within the chamber. The coupons, together with the welded I-section specimen, were placed on the bottom air baffle and just in front of the fan (where the optimum air circulation during heating was achieved), and then heated from the room temperature to each pre-specified level of elevated temperature with the applied heating rate equal to 8 ºC/min. Upon attainment of the target temperature, it was maintained for 60 min (i.e. soaking time), in order to achieve stable and uniform surface temperatures of the heated coupons and specimen [15,16]. The furnace was then switched off after the soaking period, and the coupons and specimen were naturally cooled down to the room temperature. Two thermocouples were attached to the S690 high strength steel welded I-section specimen and coupons (see Fig. 2) to monitor their actual surface temperatures during the heating, soaking and cooling processes. Fig. 3 depicts the temperature–time curves, recorded by the two thermocouples, for a typical group of coupons and specimen.

The examined grade S690 high strength steel exhibited notable change in surface colour after exposure to elevated temperatures, as evident in Fig. 4. The surface colours of S690 high strength steel after exposure to elevated temperatures of 300 ºC and 600 ºC became light brown. After exposed to higher levels of temperatures of 700 ºC and 800 ºC, the surface colours of S690 high strength steel turned into pale orange and dark red, respectively, while grey surface colour was observed for S690 high strength steel after exposure to even higher temperatures of 900 ºC and 950 ºC. The change in surface colour of S690 high strength steel after exposure to different levels of elevated temperatures can be attributed to the formation of oxide layers with different thicknesses during heating [17,18], which reflect different wavelengths of light from the steel surfaces at room temperature.

2.3. Post-fire material tensile coupon tests

Upon completion of the heating, soaking and cooling processes, the longitudinal and transverse coupons were tested in a Schenck 250 kN testing machine, to derive the material stress–strain curves and key material properties of grade S690 high strength steel after exposure to various levels of elevated temperatures. A displacement-controlled loading scheme was used to drive the actuator of the testing machine; the loading rate was initially set to be equal to 0.05 mm/min up to the predicted yield stress, while a faster rate equal to 0.8 mm/min was employed for the post-yield stage, complying with the requirements in EN ISO 6892-1 [14]. Fig. 5 depicts the material tensile coupon test rig, including two strain gauges attached to the mid-height of the coupon and an extensometer mounted onto the coupon over the central 50 mm.

The measured material stress–strain curves of the longitudinal and transverse coupons at room temperature and after exposure to various levels of elevated temperatures are plotted in Figs 6 and 7, respectively. In comparison with the room temperature material stress–strain histories, the post-fire stress–strain responses of S690 high strength steel exhibit longer yield plateaux and enhanced material ductility, though accompanied by reductions in material ultimate stresses, as also observed in previous experimental studies [11–13] on the post-fire material properties of S690 high strength steel. Table 1(a) reports the key measured material properties at room temperature, including the Young's modulus E, the yield stress f_y and the ultimate stress f_u, while Table 1(b) presents the derived key material properties of the tensile coupons after exposure to elevated temperatures, where E_T, $f_{y,T}$ and $f_{u,T}$ respectively denote the post-fire Young's modulus, yield stress and ultimate stress. It is worth noting that given that no distinct yield plateau was observed in the stress–strain curves at room temperature, the 0.2% proof stress was taken as the room temperature yield stress, whereas the stress corresponding to the yield plateau was defined as the post-fire yield stress at each level of elevated temperature.

2.4. Post-fire membrane residual stress measurements

Welded steel sections generally contain high levels of membrane residual stresses [19–23], which are introduced during the welding process and can lead to premature failure of steel structural members. For welded steel sections after exposure to elevated temperatures, the heating, soaking and cooling processes can greatly influence the patterns and amplitudes of membrane residual stresses. Therefore, the membrane residual stresses in S690 high strength steel welded I-sections after exposure to elevated temperatures were measured herein. Membrane residual stress measurements were performed by means of the sectioning method [3,23], with the procedures complying with those given in Ziemian [24]. Figs 8 and 9 schematically depict the dimensions and locations of the strips (to be sectioned) within a S690 high strength steel welded I-section specimen; the nominal width and length of each strip are respectively equal to 9 mm and 150 mm. Prior to sectioning, an automatic dot puncher was used to drill a pair of gauge holes (2 mm in diameter), located along the centreline of the outer face of each strip and at a distance of 25 mm from the strip ends; this resulted in the nominal strip length between each pair of gauge holes L_0 equal to 100 mm, while the actual length between the two gauge holes for each strip within the intact S690 high strength steel welded I-section specimens was measured by means of a Demec gauge. The welded I-section specimens were then sectioned into strips to allow for the release of membrane residual stresses; this was achieved by using a waterjet cutting machine, which resulted in very little additional heat input during cutting, therefore ensuring that the original patterns and amplitudes of membrane residual stresses in S690 high strength steel welded I-sections remained generally unaltered. A typical sectioned S690 high strength steel welded I-section specimen is presented in Fig. 10. Upon completion of the sectioning process, the Demec gauge was employed again to measure the length of each strip between the two gauge holes. In order to capture the influence of temperature variation on the change in strip lengths, a temperature reference bar, cut from the same batch of S700MC high strength steel sheets as that used for fabricating the S690 high strength steel welded I-section specimens, was utilised. Two gauge holes were also drilled on the temperature reference bar, and its length between the gauge holes was firstly measured by the Demec gauge on the same day when length measurements of the strips within the intact S690 high strength steel welded I-sections were conducted, and then also recorded on the same day when length measurements of the strips sectioned from the S690 high strength steel welded I-sections were performed.

The relived axial strain of each sectioned strip ε_0 (as a result of the released membrane residual stress) can be calculated from Eq. (1), in which r_1 and r_2 are the strip lengths as measured from the Demec gauge respectively before and after sectioning of the S690 high strength steel welded I-section, and t_1 denotes the length of the temperature reference bar recorded on the same day when length measurement of the strip within the intact S690 high strength steel welded I-section is carried out, while t_2 denotes the length of the temperature reference bar recorded on the same day when length measurement of the strip sectioned from the S690 high strength steel welded I-section is performed; negative and positive values of ε_0 derived from Eq. (1) stand for compressive and tensile axial strains relieved during the sectioning process, respectively. It is worth noting that the sectioned strips in the vicinity of welds displayed slightly curved shapes; this can be attributed to the existence of a relatively high level of through-thickness bending residual stresses near the welds, and corrections to the relieved axial strains calculated from Eq. (1) were then made based on Eq. (2) [3,23,25], in which δ is the maximum deviation measured from a straight reference line connecting the two gauge holes of the curved strip and $\varepsilon_{0,c}$ is the corrected relieved axial strain. The released membrane residual stress for each strip can then be back-calculated as the relieved axial strain (ε_0 or $\varepsilon_{0,c}$) multiplied by the corresponding material modulus of elasticity (E for strips cut from the unheated S690 high strength steel welded I-section specimen and E_T for strips sectioned from the S690 high strength steel welded I-section specimens after exposure to elevated temperatures – see Table 3); note that negative and positive values respectively indicate compressive and tensile membrane residual stresses.

$$\varepsilon_0 = \frac{(r_1 - t_1) - (r_2 - t_2)}{L_0 + (r_1 - t_1)} \tag{1}$$

$$\varepsilon_{0,c} = \varepsilon_0 + \frac{(\delta/L_0)^2}{6(\delta/L_0)^4 + 1} \tag{2}$$

The patterns and amplitudes of the measured membrane residual stresses in S690 high strength steel welded I-sections at room temperature and after exposure to various levels of elevated temperatures are plotted in Figs 11(a)–11(g). The ratios of the measured peak tensile and compressive membrane residual stresses to the corresponding material yield stresses are reported in Table 2, in which $f_{t,T}$ (or f_t) signifies the post-fire (or room temperature) peak tensile membrane residual stress, while $f_{c,T}$ (or f_c) denotes the post-fire (or room temperature) peak compressive membrane residual stress.

3. Discussion and analysis of key post-fire material properties of S690 high strength steel

3.1. General

The experimentally derived key post-fire residual material properties of S690 high strength steel were fully discussed and then compared with the corresponding room temperature material properties in this section. Table 3 presents the measured post-fire retention factors of the Young's modulus (E_T/E), yield stress ($f_{y,T}/f_y$) and ultimate stress ($f_{u,T}/f_u$), while the retention factors of these key material properties are plotted against the temperatures in Figs 12–14, where three sets of relevant experimental data collected from Qiang et al. [11], Li et al. [12] and Li and Young [13] are also located, together with the corresponding proposed retention factor curves. The accuracy and efficiency of these previously proposed retention factor curves were firstly evaluated, based on the measured and collected data, followed by the development of more simple but still accurate retention factor curves.

3.2. Post-fire retention factor for Young's modulus

The post-fire retention factors for the Young's modulus E_T/E, as measured in the present study and collected from Qiang et al. [11], Li et al. [12] and Li and Young [13], are plotted against the temperatures in Fig. 12. The measured Young's moduli of S690 high strength steel remain almost unchanged (i.e. the E_T/E ratios are approximately equal to unity) for elevated temperatures up to around 500 ºC, but decrease thereafter. This trend is also followed by the Young's modulus retention factors for S690 high strength steel collected from Qiang et al. [11] Li et al. [12] and Li and Young [13], though the data points of Qiang et al. [11] are distinctly lower for temperatures above around 600 ºC. The post-fire retention factor curves for the Young's modulus of S690 high strength steel, as proposed in Qiang et al. [11], Li et al. [12] and Li and Young [13], are defined by Eqs (3)–(5), respectively, and also plotted in Fig. 12. The results of the graphic evaluation indicated that all the three proposed retention factor curves well represent the measured and collected data for temperatures up to around 500 ºC; regarding higher levels of temperatures beyond 500 ºC, the two retention factor curves of Qiang et al. [11] and Li and Young [13] provide lower bounds to the experimental data, while the retention factor curve of Li et al. [12], as proposed and calibrated based only on its own test data, was shown to overestimate other sets of measured post-fire Young's moduli.

$$\frac{E_T}{E} = \begin{cases} -1.52\times10^{-10}\times T^3 + 2.7\times10^{-8}\times T^2 - 3.35\times10^{-5}\times T + 1 & 20 \le T \le 600 \\ 6.27\times10^{-9}\times T^3 - 1.38\times10^{-5}\times T^2 + 8.95\times10^{-3}\times T - 0.806 & 600 < T \le 1000 \end{cases} \quad (3)$$

$$\frac{E_T}{E} = 1 \qquad 20 \le T \le 900 \quad (4)$$

$$\frac{E_T}{E} = \begin{cases} 1 - \dfrac{T-20}{20000} & 20 < T \le 600 \\ 0.971 - \dfrac{T-600}{950} & 600 < T \le 900 \\ 0.655 - \dfrac{T-900}{10000} & 900 < T \le 1000 \end{cases} \tag{5}$$

3.3. Post-fire retention factor for yield stress

The measured retention factors for the material yield stress of S690 high strength steel $f_{y,T}/f_y$, together with those reported in Qiang et al. [11], Li et al. [12] and Li and Young [13], are displayed in Fig. 13, in which the post-fire yield stresses of S690 high strength steel are generally shown to increase for elevated temperatures up to around 500 ºC to 600 ºC, but decrease rapidly for higher levels of temperatures. The corresponding retention factor curves of Qiang et al. [11], Li et al. [12] and Li and Young [13], as respectively defined by Eqs (6)–(8), are also plotted in Fig. 13, with their accuracy assessed against the four sets of experimental data points. The graphical assessment results indicated that (i) the retention factor curve proposed by Qiang et al. [11] greatly overestimates the post-fire yield stresses for temperatures above around 600 ºC, (ii) the retention factor curve of Li et al. [12] generally follows the trend of the measured and collected test data but slightly overestimates the post-fire yield stresses for temperatures greater than about 700 ºC, and (iii) the retention factor curve given in Li and Young [13] leads to safe predictions of post-fire yield stresses over the full temperature range except for one test data. Given that all the three yield stress retention factor curves were defined by complicated functions of nonlinear polynomial forms and showed some shortcomings, a new simple multi-linear predictive curve is proposed herein, as given by Eq. (9), and also shown to be capable of accurately predicting the post-fire material yield stresses of S690 high strength steel in Fig. 13.

$$\frac{f_{y,T}}{f_y} = \begin{cases} 1 - \dfrac{(T-20)^{1.584}}{9957 \times T} & 20 \le T < 650 \\ 1.8 \times 10^{-8} \times T^3 - 4.03 \times 10^{-5} \times T^2 + 2.74 \times 10^{-2} \times T - 4.711 & 650 \le T \le 1000 \end{cases} \quad (6)$$

$$\frac{f_{y,T}}{f_y} = \begin{cases} 1 & 20 \le T < 500 \\ 1.693 \times 10^{-6} \times T^2 - 0.003687 \times T + 2.42 & 500 \le T \le 900 \end{cases} \quad (7)$$

$$\frac{f_{y,T}}{f_y} = \begin{cases} 1 - \dfrac{T-20}{30000} & 20 < T \le 500 \\ 0.984 - \dfrac{(T-500)^{2.5}}{1600000} & 500 < T \le 750 \\ 0.366 - \dfrac{T-750}{100000} & 750 < T \le 1000 \end{cases} \quad (8)$$

$$\frac{f_{y,T}}{f_y} = \begin{cases} 1 & 30 \le T \le 500 \\ 1 - \dfrac{21 \times (T-500)}{10000} & 500 < T \le 800 \\ 0.37 & 800 < T \le 1000 \end{cases} \quad (9)$$

3.4. Post-fire retention factor for ultimate stress

The retention factors for the material ultimate stress derived from the tensile coupon tests, in combination with the three sets of previously measured retention factors by Qiang et al. [11], Li et al. [12] and Li and Young [13], are plotted against the temperatures in Fig. 14. It was found that the post-fire ultimate stresses of S690 high strength steel generally remain unchanged (i.e. the $f_{u,T}/f_u$ ratios are approximately equal to unity) for temperatures up to around 500 ºC, but exhibit an decreasing trend at higher temperatures. The ultimate stress retention factor curves, as proposed in Qiang et al. [11], Li et al. [12] and Li and Young [13], are defined by Eqs (10)–(12), respectively, and are also presented in Fig. 14. The measured and collected post-fire ultimate stress retention factors for temperatures up to around 400 ºC are generally well captured by the curve reported in Qiang et al. [11], but a high level of scatter was found when the predictive curve was adopted to determine the retention factors for elevated temperatures beyond 400 ºC, i.e. with unsafe predictions for elevated temperatures ranging from 400 ºC to 600 ºC and conservative predictions for higher elevated temperatures. The retention factor curve proposed in Li et al. [12] was shown to well capture the post-fire ultimate stress data points for temperatures up to about 600 ºC, as evident in Fig. 14; however, the curve lies above the data points at higher temperatures (i.e. resulting in unsafe post-fire ultimate stress predictions). The predictive curve of Li and Young [13], was found to overly underestimate the post-fire material ultimate stresses of S690 high strength steel across almost the full range of elevated temperatures. Given that all the three ultimate stress retention factor curves were defined by complicated functions of nonlinear polynomial forms and showed some shortcomings, a new curve of simple multi-linear shape, as expressed by Eq. (13), was developed for predicting the post-fire ultimate stresses of S690 high strength steel, and is also plotted in Fig. 14, revealing a good level of accuracy.

$$\frac{f_{u,T}}{f_u} = \begin{cases} 1 & 20 \le T \le 600 \\ -1.24\times10^{-10}\times T^4 + 4.13\times10^{-7}\times T^3 - 5.077\times10^{-4}\times T^2 + 0.271\times T - 52.21 & 600 < T \le 1000 \end{cases} \tag{10}$$

$$\frac{f_{u,T}}{f_u} = \begin{cases} 1 & 20 \le T < 400 \\ 4.102\times10^{-7}\times T^2 - 0.001356\times T + 1.477 & 400 \le T \le 900 \end{cases} \tag{11}$$

$$\frac{f_{u,T}}{f_u} = \begin{cases} 1 - \dfrac{(T-20)^{2.5}}{29000000} & 20 < T \le 750 \\ 0.504 - \dfrac{T-750}{12000} & 750 < T \le 1000 \end{cases} \tag{12}$$

$$\frac{f_{u,T}}{f_u} = \begin{cases} 1 & 30 \le T \le 500 \\ 1 - \dfrac{7 \times (T - 500)}{4000} & 500 < T \le 800 \\ 0.475 & 800 < T \le 1000 \end{cases} \qquad (13)$$

4. Discussion and analysis of post-fire membrane residual stresses in S690 high strength steel welded I-sections

4.1. Measured post-fire membrane residual stresses in S690 high strength steel welded I-sections

The patterns and amplitudes of the measured membrane residual stresses in S690 high strength steel welded I-sections after exposed to elevated temperatures were thoroughly analysed in this section. It is evident in Figs 11(a) and 11(b) that the membrane residual stress pattern and amplitudes in S690 high strength steel welded I-section after exposed to an elevated temperature of 300 ºC generally remain unchanged in comparison with those in S690 high strength steel welded I-section at room temperature. After exposed to a higher level of elevated temperature of 600 ºC, S690 high strength steel welded I-section, however, experiences a sharp decrease in membrane residual stress magnitudes, and the difference between the peak tensile and compressive membrane residual stress magnitudes for each constituent plate element also becomes smaller – see Fig. 11(c). This can be attributed to the fact that thermal creep of steel becomes significant when temperature reaches 500 ºC–600 ºC [26,27], and results in prominent reduction and redistribution of elastic strains throughout the cross-section. The occurrence of elastic strain reduction and redistribution induces a high level of residual stress relaxation, and finally leads to reductions in membrane residual stress magnitudes and lessens the discrepancy between the peak tensile and compressive membrane residual stress magnitudes. Regarding S690 high strength steel welded I-sections after exposure to even higher elevated temperatures from 700 ºC to 950 ºC, their membrane residual stress magnitudes decrease slightly (compared to those of S690 high strength steel welded I-sections after exposure to an elevated temperature of 600 ºC), since most of the residual stress relaxation occurs at 500 ºC–600 ºC [26,27], and the discrepancy between the peak tensile and compressive membrane residual stress magnitudes for each constituent plate element becomes even smaller, as shown in Figs 11(d)–11(g).

4.2. Assessment of codified membrane residual stress predictive models for mild steel welded I-sections at room temperature

Given that there have been no predictive models for predicting the patterns and amplitudes of membrane residual stresses in S690 high strength steel welded I-sections at room temperature and after exposure to fire, the applicability of two membrane residual stress predictive models for mild steel welded I-sections at room temperature, as given in the European convention ECCS [28] and Swedish regulations BSK 99 [29], was assessed for the post-fire membrane residual stresses in S690 high strength steel welded I-sections. The two considered membrane residual stress predictive models were developed based on the same distribution pattern – see Fig. 15, but with different amplitudes of peak membrane residual stresses and distribution parameters (a, b, c and d), as given in Table 4. Note that the magnitudes of the peak tensile membrane residual stresses prescribed in both of the two predictive models are equal to the material yield stress f_y, while the magnitudes of the peak compressive membrane residual stresses are defined as $0.25f_y$ in ECCS [28] but derived from self-equilibrium in BSK 99 [29]. For S690 high strength steel welded I-section at room temperature or after exposure to each level of elevated temperature, the measured membrane residual stresses of the flanges and web are normalised with respect to the corresponding room temperature or post-fire yield stress, and plotted against the normalised positions, with the origin point (0.0) and end point (1.0) respectively standing for the web-to-flange junction and the flange tip (or web mid-point), as depicted in Figs 16–22. The two predicted models are also plotted in Figs 16–22, enabling direct graphical comparisons against the measured room temperature and post-fire membrane residual stresses. The results of the graphical comparisons generally revealed that the two considered predictive models overestimate the peak tensile residual stresses but underestimate the peak compressive residual stresses in S690 high strength steel welded I-sections at room temperature of 30 ºC and after exposure to an elevated temperature of 300 ºC; regarding S690 high strength steel welded I-sections after exposure to higher temperatures ranging from 600 ºC to 950 ºC, all the normalised peak tensile membrane residual stress values ($f_{t,T}/f_{y,T}$) are less than 0.2, which are excessively overestimated by the two considered predictive models. Overall, the two existing predictive models for membrane residual stresses in mild steel welded I-sections at room temperature are not capable of representing those in S690 high strength steel welded I-sections at room temperature and after exposure to elevated temperatures.

4.3. Development of new membrane residual stress predictive model for S690 high strength steel welded I-sections after exposure to elevated temperatures

A new predictive model capable of predicting the post-fire membrane residual stress patterns and amplitudes in S690 high strength steel welded I-sections was proposed herein based on the experimentally measured data. The proposed predictive model follows the general distribution pattern as shown in Fig. 15, but adopts different sets of distribution parameters and peak membrane residual stress amplitudes for different elevated temperatures. Specifically, for S690 high strength steel welded I-sections after exposure to elevated temperatures lower than 500 ºC (i.e. without the occurrence of prominent residual stress relaxation), it was proposed that the membrane residual stress predictive model, as recommend in Sun et al. [3] for S690 high strength steel welded I-sections at room temperature, be employed, but with the post-fire yield stress replacing the room temperature yield stress in the calculation of the peak tensile membrane residual stresses, i.e. $0.8f_{y,T}$, as summarised in Table 5. For S690 high strength steel welded I-sections after exposure to higher temperatures ranging from 500 ºC to 800 ºC, the peak tensile residual stresses were taken as $0.2f_{y,T}$, to take into account the effect of prominent membrane residual stress relaxation, with the proposed distribution parameters summarised in Table 5. For S690 high strength steel welded I-sections after exposure to elevated temperatures higher than 800 ºC, the peak tensile residual stresses were still given as $0.2f_{y,T}$, but with a different set of distribution parameters, as reported in Table 5. Comparisons of the membrane residual stresses in S690 high strength steel welded I-sections at room temperature and after exposure to various levels of elevated temperatures against the proposed predictive model are shown in Figs 16–22, indicating good agreement.

5. Conclusions

A thorough testing programme has been conducted to investigate the material properties and membrane residual stresses of S690 high strength steel welded I-sections after exposure to elevated temperatures. The experimental programme included heating, soaking and cooling of S690 high strength steel (longitudinal and transverse) coupon and welded I-section specimens, with the adoption of seven levels of elevated temperatures ranging from 30 ºC (i.e. room temperature) to 950 ºC, as well as post-fire material tensile coupon tests and membrane residual stress measurements. The measured post-fire material properties from the longitudinal and transverse tensile coupons were carefully analysed with those collected from previous studies [11–13]. Both the measured and collected data revealed that the post-fire Young's moduli and ultimate stresses of S690 high strength steel generally remained unchanged for temperatures up to around 500 ºC, but experienced steep reductions for higher temperatures from 500 ºC to 950 ºC, while the post-fire yield stresses of S690 high strength steel displayed an increasing trend for elevated temperatures up to about 500 ºC, but rapidly decreased with temperatures above 500 ºC. Given that the current established material post-fire retention factor curves for S690 high strength steel are defined by complicated functions of nonlinear polynomial forms and have some shortcomings, a new set of simple multi-linear retention factor curves has been proposed, and shown to lead to accurate predictions of yield and ultimate stresses for S690 high strength steel after exposure to elevated temperatures. The measured membrane residual stresses in S690 high strength steel welded I-sections after exposure to an elevated temperature of 300 ºC were found to remain generally unchanged in comparison with those in S690 high strength steel welded I-section at room temperature, while the post-fire membrane residual stresses for higher temperatures ranging from 600 ºC to 950 ºC experienced sharp decreases due to prominent residual stress relaxation. A predictive model specific for membrane residual stresses in S690 high strength steel welded I-sections after exposure to elevated temperatures has been proposed, and shown to well represent the measured membrane residual stress patterns and amplitudes over the full temperature range from 30 ºC to 950 ºC.

Acknowledgements

The authors thank SSAB Swedish Steel Pte Ltd., Singapore for helping fabricate S690 high strength steel welded I-sections, and also acknowledge the financial support from Regency Steel Asia (RSA) Endowment Fund and NTU Research Scholarship.

References

[1] D. Li, Z. Huang, B. Uy, H. Thai, C. Hou, Slenderness limits for fabricated S960 ultra-high-strength steel and composite columns, J. Constr. Steel Res. 159 (2019) 109–121.

[2] F. Wang, O. Zhao, B. Young, Flexural behaviour and strengths of press-braked S960 ultra-high strength steel channel section beams, Eng. Struct. 200 (2019) 109735.

[3] Y. Sun, Y. Liang, O. Zhao, Testing, numerical modelling and design of S690 high strength

steel welded I-section stub columns, J. Constr. Steel Res. 159 (2019) 521–533.

[4] K.J.R. Rasmussen, G.J. Hancock, Plate slenderness limits for high strength steel sections, J. Constr. Steel Res. 23 (1992) 73–96.

[5] K. Wang, Study on Structural behaviour of High Strength Steel S690 Welded H- and I-Sections, Ph.D thesis, the Hong Kong Polytechnic University, 2018.

[6] Y. Sun, A. He, Y. Liang, O. Zhao, In-plane bending behaviour and capacities of S690 high strength steel welded I-section beams, 162 (2019).

[7] K.J.R. Rasmussen, G.J. Hancock, Tests of high strength steel columns, J. Constr. Steel Res. 34 (1995) 27–52.

[8] T. Li, G. Li, S. Chan, Y. Wang, Behavior of Q690 high-strength steel columns: Part 1: Experimental investigation, J. Constr. Steel Res. 123 (2016) 18–30.

[9] G. Shi, H. Ban, F.S.K. Bijlaard, Tests and numerical study of ultra-high strength steel columns with end restraints, J. Constr. Steel Res. 70 (2012) 236–247.

[10] T. Ma, Y. Hu, X. Liu, G. Li, K.F. Chung, Experimental investigation into high strength Q690 steel welded H-sections under combined compression and bending, J. Constr. Steel Res. 138 (2017) 449–462.

[11] X. Qiang, F.S.K. Bijlaard, H. Kolstein, Post-fire mechanical properties of high strength structural steels S460 and S690, Eng. Struct. 35 (2012) 1-10.

[12] G. Li, H. Lyu, C. Zhang, Post-fire mechanical properties of high strength Q690 structural steel, J. Constr. Steel Res. 132 (2017) 108-116.

[13] H. Li, B. Young, Residual mechanical properties of high strength steels after exposure to fire, J. Constr. Steel Res. 148 (2018) 562-571.

[14] EN ISO 6892-1, Metallic Materials: Tensile Testing - Part 1: Method of Test at Room Temperature, European Committee for Standardization (CEN), Brussels, 2016.

[15] Y. Huang, B. Young, Post-fire behaviour of ferritic stainless steel material, Constr. Build. Mater. 157 (2017) 654–667.

[16] A. He, Y. Liang, O. Zhao, Experimental and numerical studies of austenitic stainless steel CHS stub columns after exposed to elevated temperatures, J. Constr. Steel Res. 154 (2019) 293–305.

[17] G.Cao, V.Firouzdor, K.Sridharan, M. Anderson, T.R. Allen, Corrosion of austenitic alloys in high temperature supercritical carbon dioxide, Corrosion Science 60 (2012) 246-255.

[18] S.E. Ziemniak, M. Hanson, Corrosion behavior of 304 stainless steel in high temperature, hydrogenated water, Corrosion Science 44 (2002) 2209-2230.

[19] H. Ban, G. Shi, Y. Shi, Y. Wang, Residual stress of 460 MPa high strength steel welded box section : Experimental investigation and modeling, Thin Walled Struct. 64 (2013) 73–82.

[20] X. Liu, K.F. Chung, Experimental and numerical investigation into temperature histories and residual stress distributions of high strength steel S690 welded H-sections, Eng. Struct. 165 (2018) 396-411.

[21] H. Yuan, Y. Wang, Y. Shi, L. Gardner, Residual stress distributions in welded stainless steel sections. Thin-walled Struct 79 (2014) 38–51.

[22] L. Gardner, Y. Bu, M. Theofanous, Laser-welded stainless steel I-sections : Residual stress measurements and column buckling tests, Eng. Struct. 127 (2016) 536–548.

[23] Y. Sun, O. Zhao, Material response and local stability of high-chromium stainless steel welded I-sections, Eng. Struct. 178 (2019) 212-226.

[24] R.D. Ziemian, Guide to Stability Design Criteria for Metal Structures, 6th ed. John Wiley & Sons, 2010.

[25] N. Tebedge, G. Alpsten, L. Tall, Residual-stress Measurement by the Sectioning Method, Exp. Mech. 13 (2) (1973) 88–96.

[26] J. Brnic, G. Turkalj, M. Canadija, D. Lanc, Creep behavior of high-strength low-alloy steel at elevated temperatures, Material Science and Engineering A 499 (2009) 23–27.

[27] W. Wang, G. Li, Y. Ge, Residual stress study on welded section of high strength Q460 steel after fire exposure, Advanced Steel Construction 11 (2015) 150–164.

[28] ECCS, European Convention For Constructional Steelwork: convention Europeenne de la construction metallique, 1976.

[29] BSK 99, Swedish regulations for steel structures, Boverks Handbok Om Stalkonstructioner, Karlskrona, Sweden. 1999.

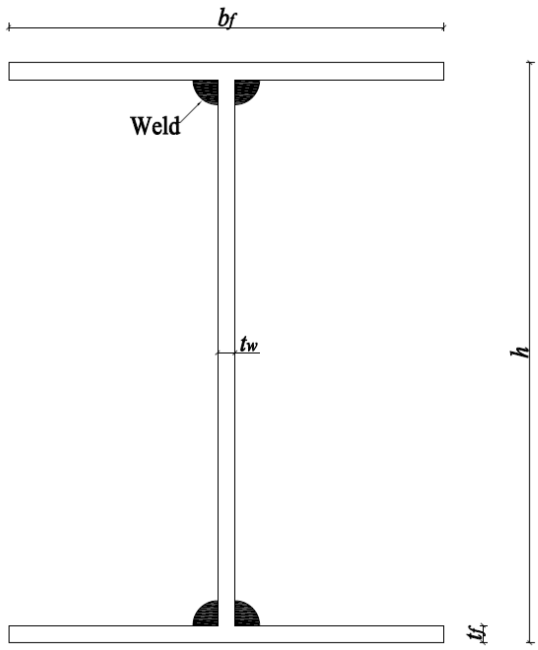

Fig. 1. Notations of welded I-section.

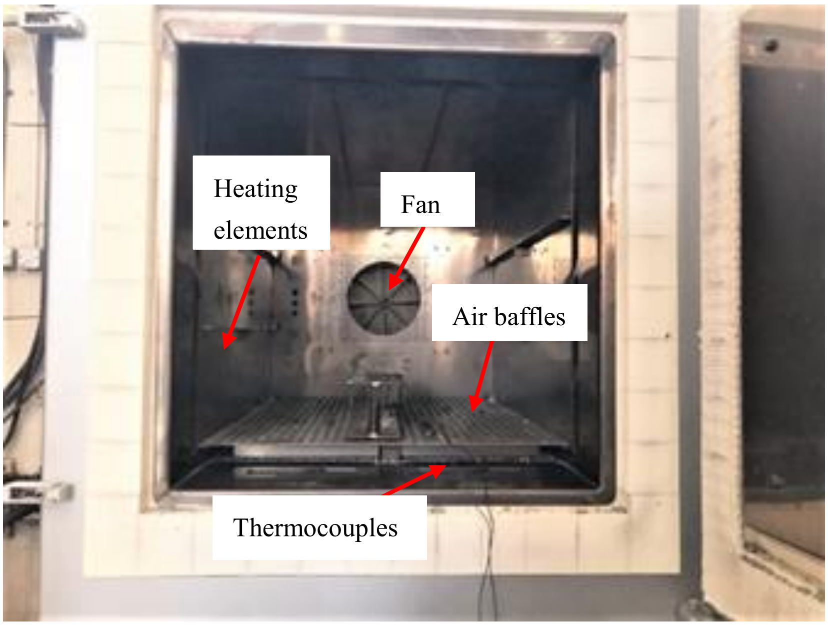

Fig. 2. Nabertherm forced convection chamber furnace.

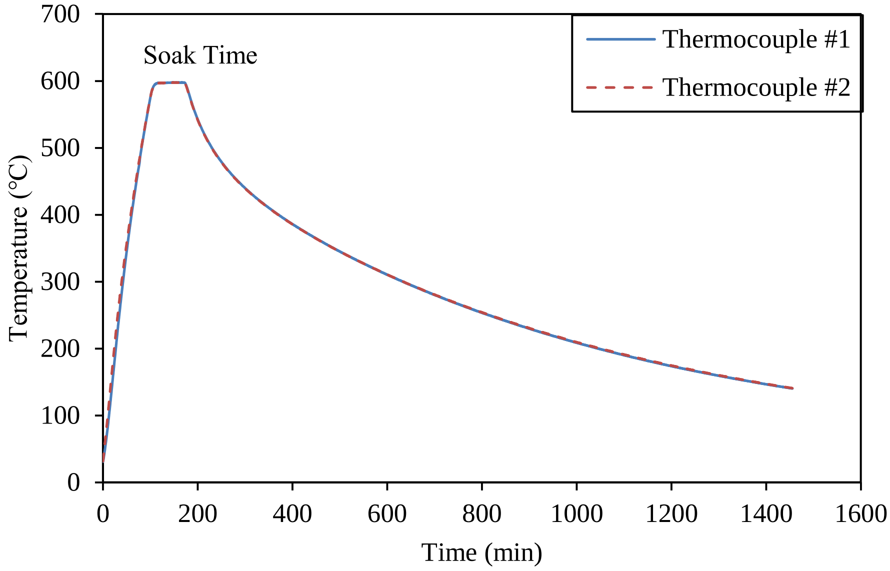

Fig. 3. Temperature–time curves for a typical group of coupons and specimen during heating, soaking and cooling processes.

Fig. 4. S690 high strength steel longitudinal coupons at room temperature and after exposure to different levels of elevated temperatures.

Fig. 5. Tensile coupon test setup.

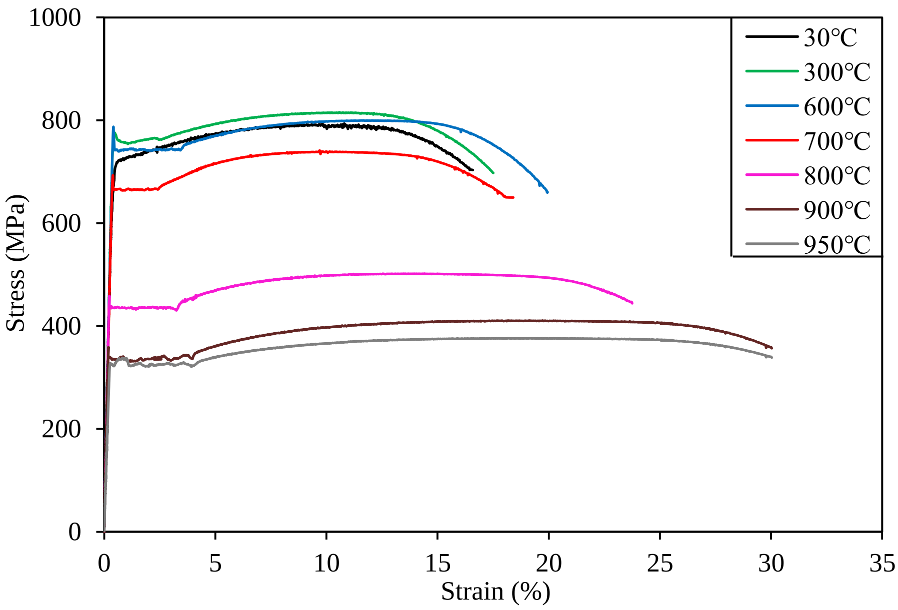

Fig. 6. Stress–strain curves of S690 high strength steel longitudinal coupons at room temperature and after exposure to different levels of elevated temperatures.

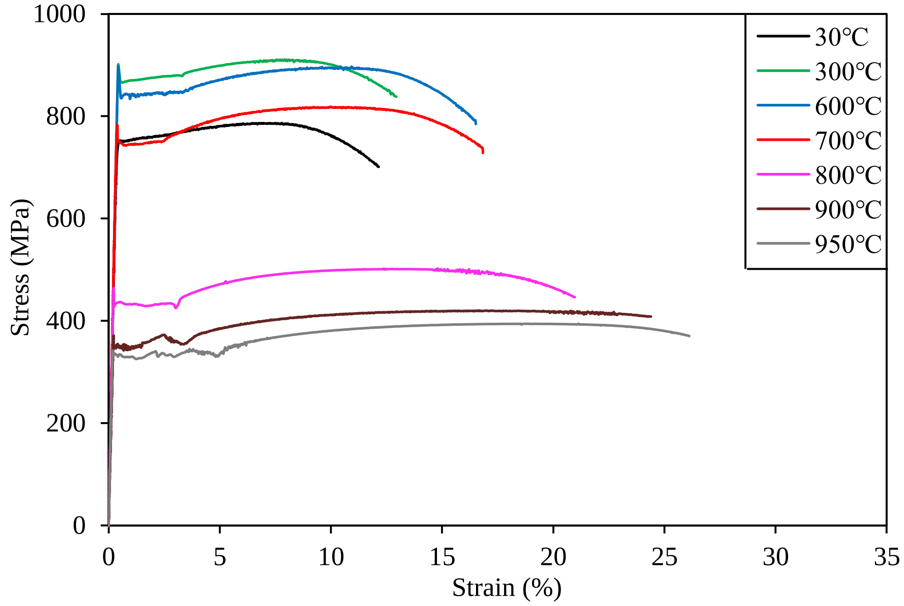

Fig. 7. Stress–strain curves of S690 high strength steel transverse coupons at room temperature and after exposure to different levels of elevated temperatures.

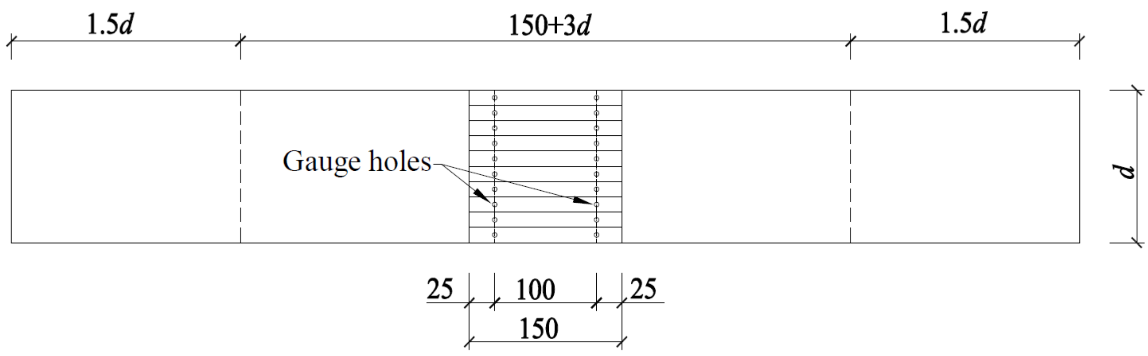

Fig. 8. Location of strips cut for residual stress measurements (dimension in millimeters).

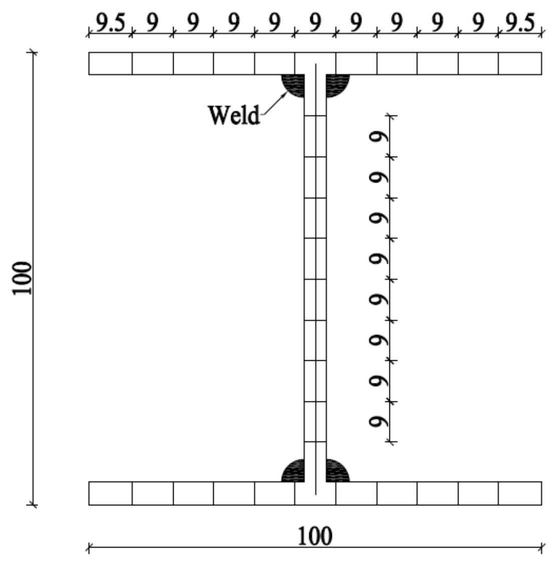

Fig. 9. Locations and dimensions of strips within S690 high strength steel welded I-section (dimension in millimeters)

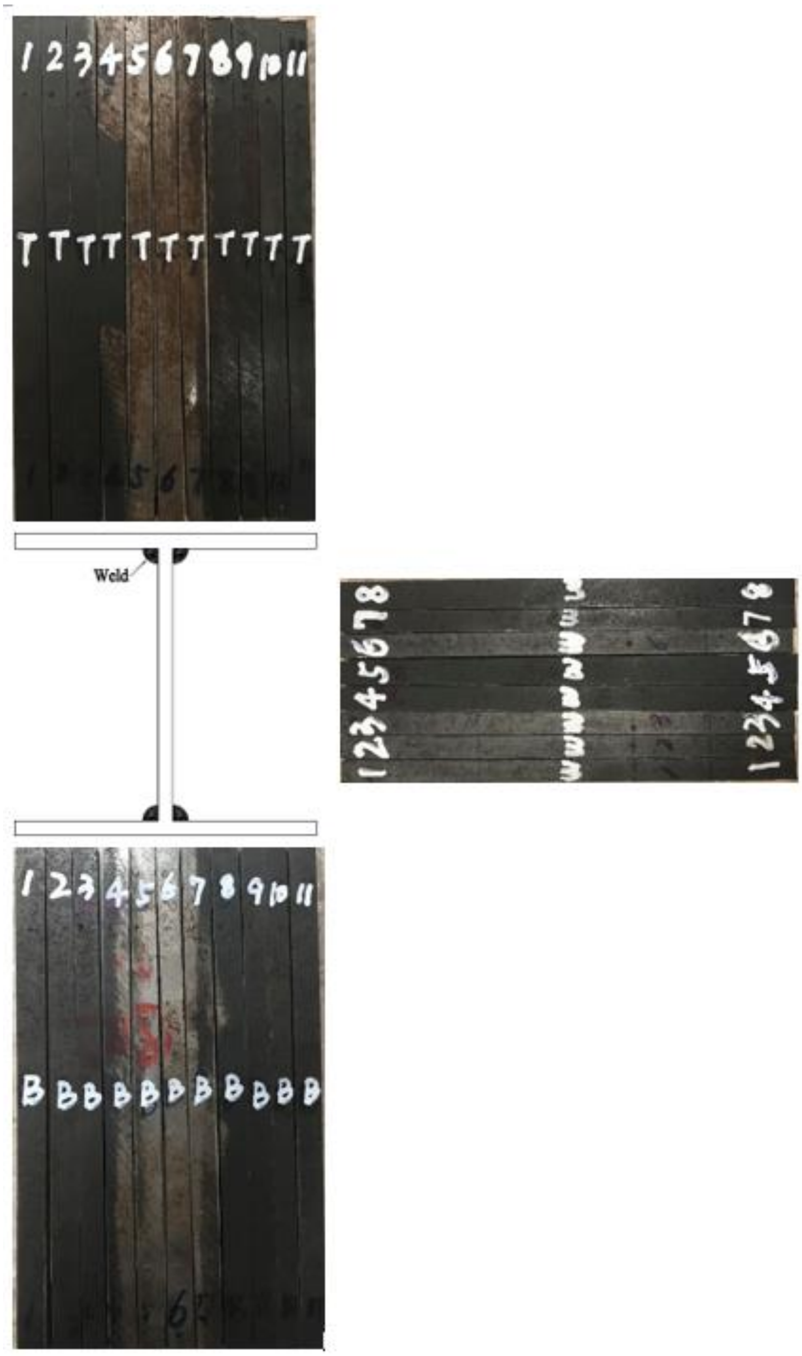

Fig. 10. Typical sectioned S690 high strength steel welded I-section specimen.

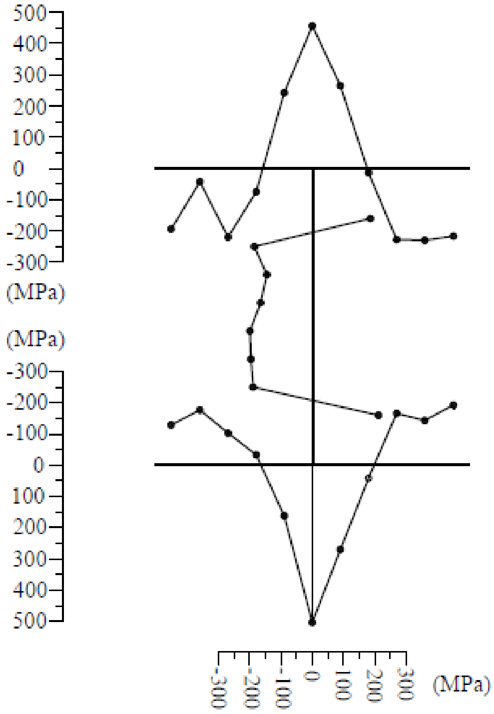

(a) T=30 ℃

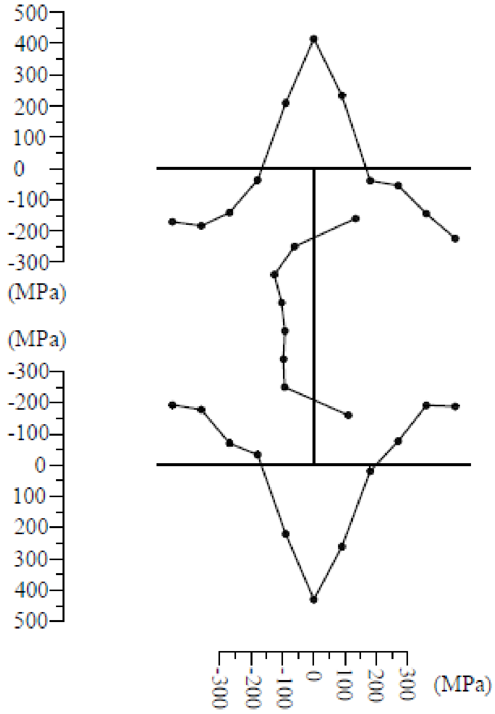

(b) T=300 ℃

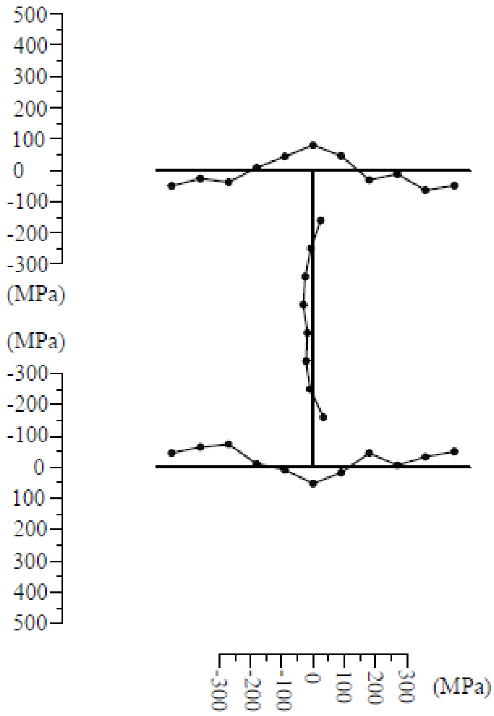

(c) T=600 ℃

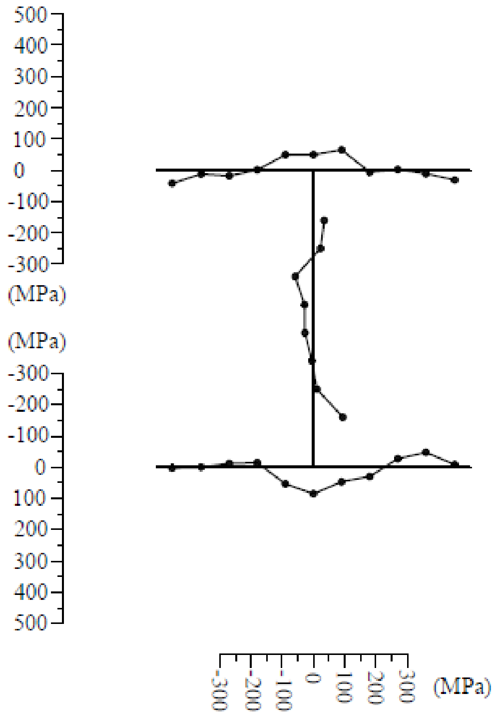

(d) T=700 ℃

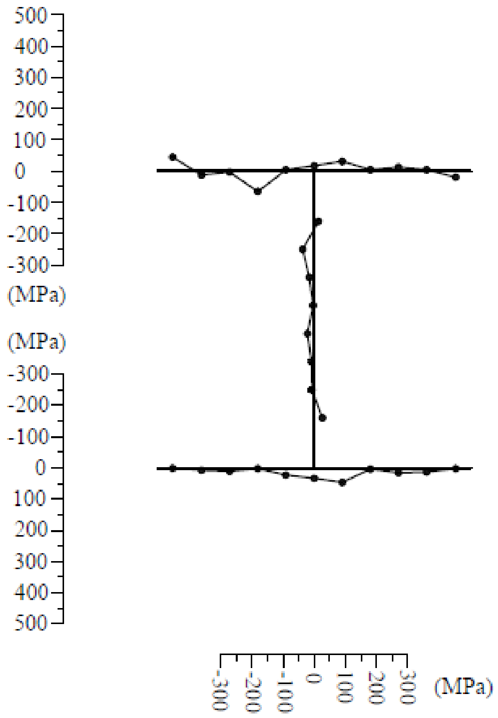

(e) T=800 ℃

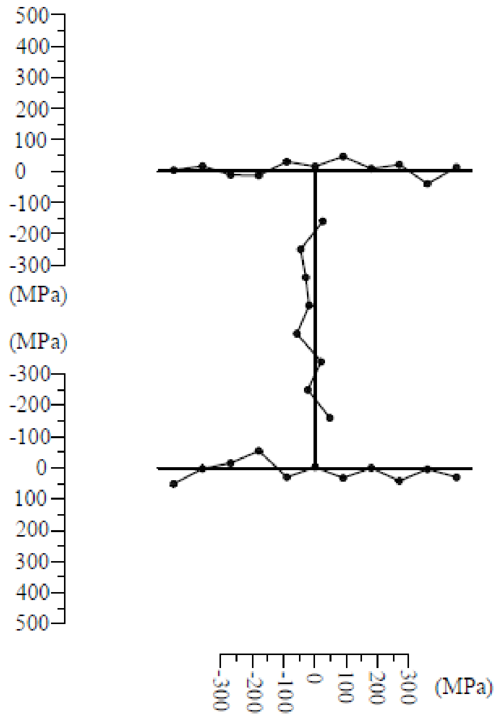

(f) T=900 ℃

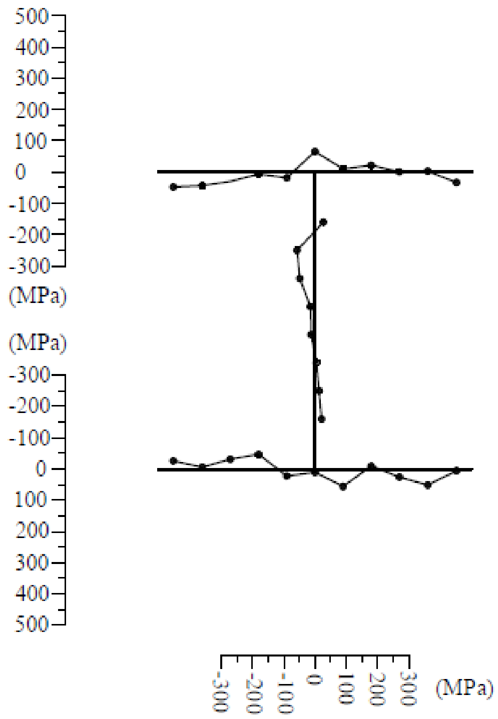

(g) T=950 ℃

Fig. 11. Measured membrane residual stress patterns and amplitudes for S690 high strength steel welded I-sections at room temperature and after exposure to different levels of elevated temperatures.

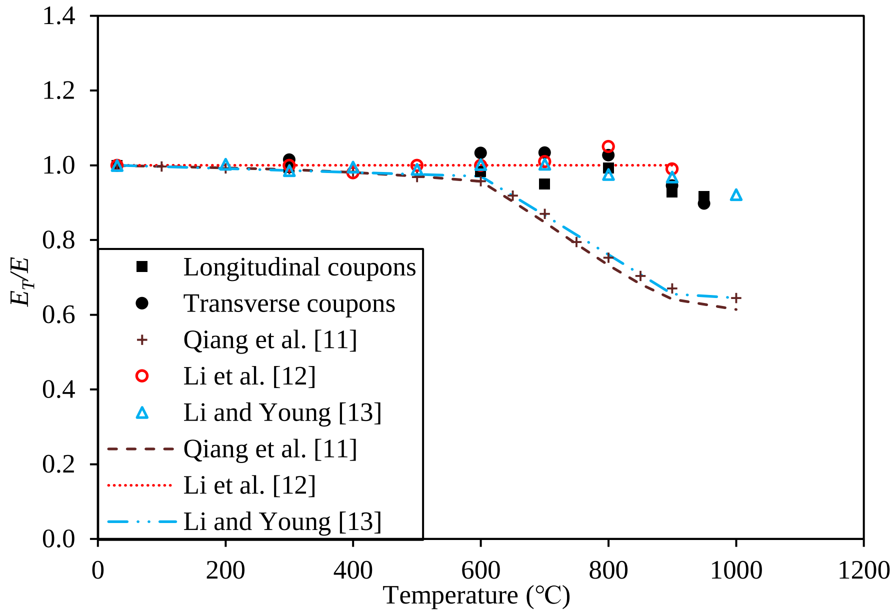

Fig. 12. Retention factors for Young's modulus.

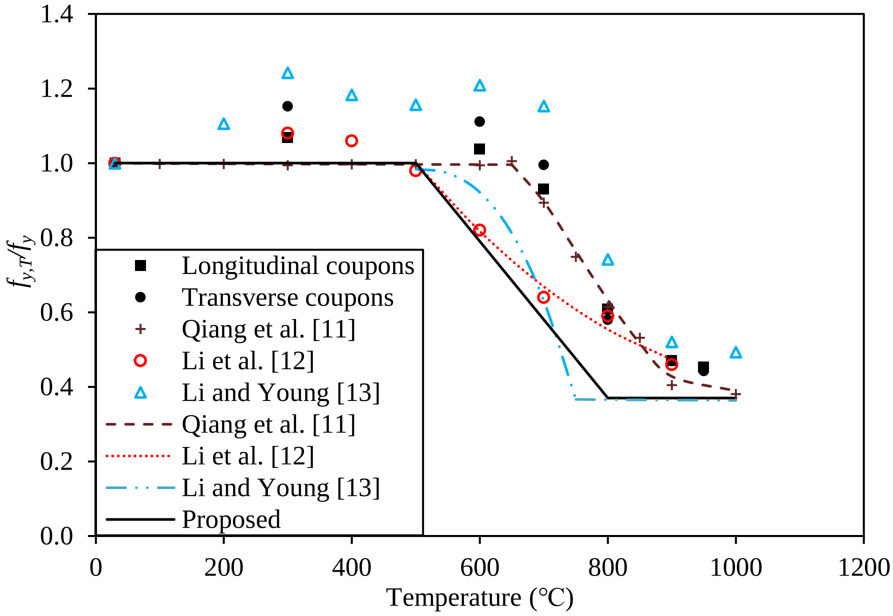

Fig. 13. Retention factors for yield stress.

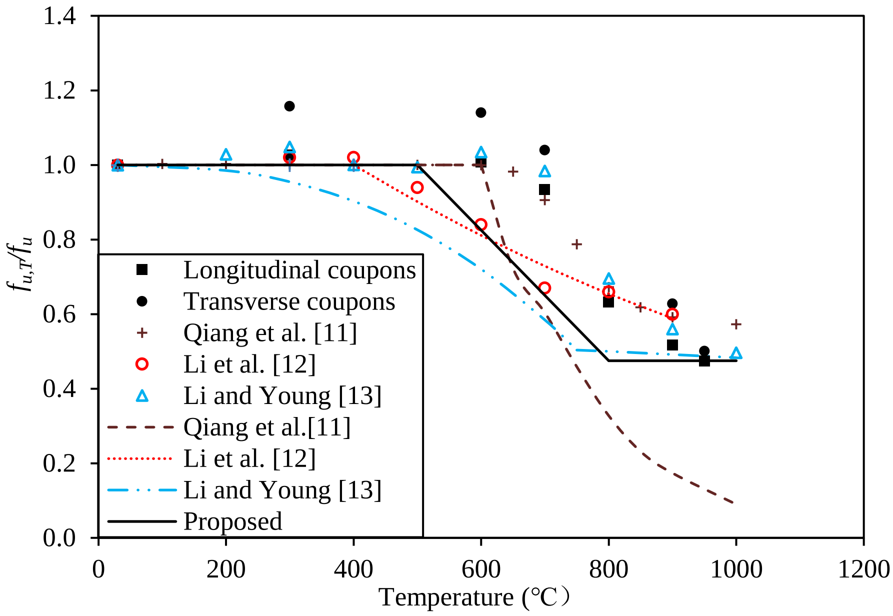

Fig. 14. Retention factors for ultimate stress.

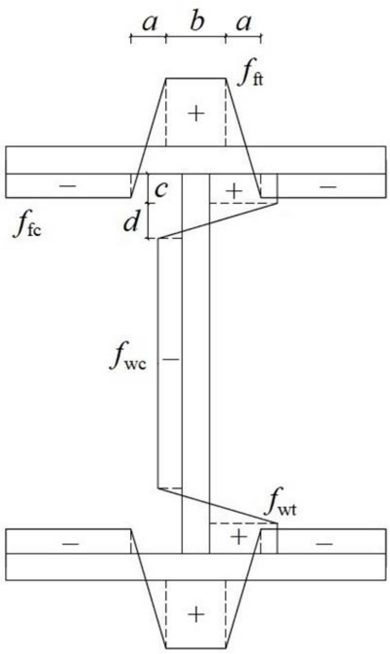

Fig. 15. Membrane residual stress distribution pattern for welded I-sections.

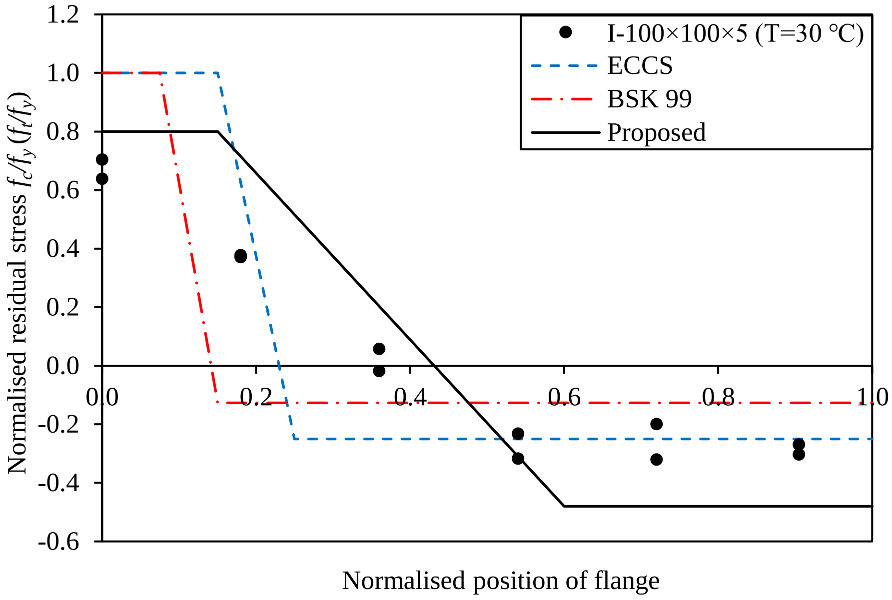

(a) Flange (T=30 °C)

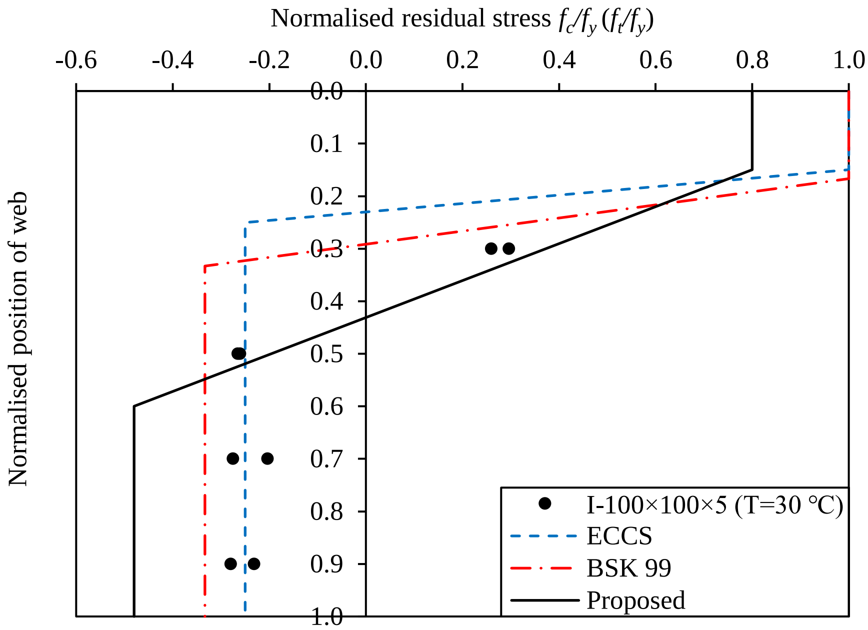

(b) Web (T=30 °C)

Fig. 16. Comparisons between measured residual stresses in S690 high strength steel welded I-section at room temperature (T=30 °C) and predictive models.

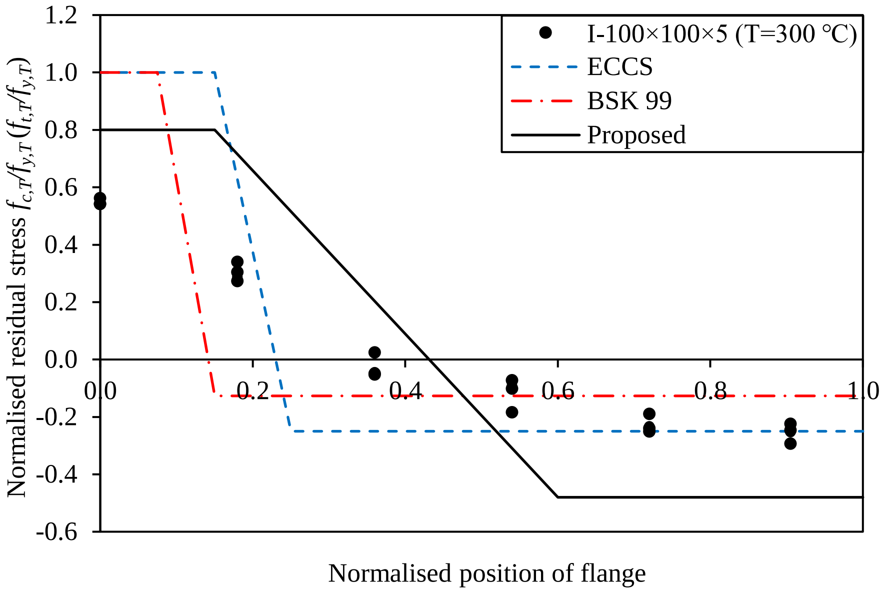

(a) Flange (T=300 °C)

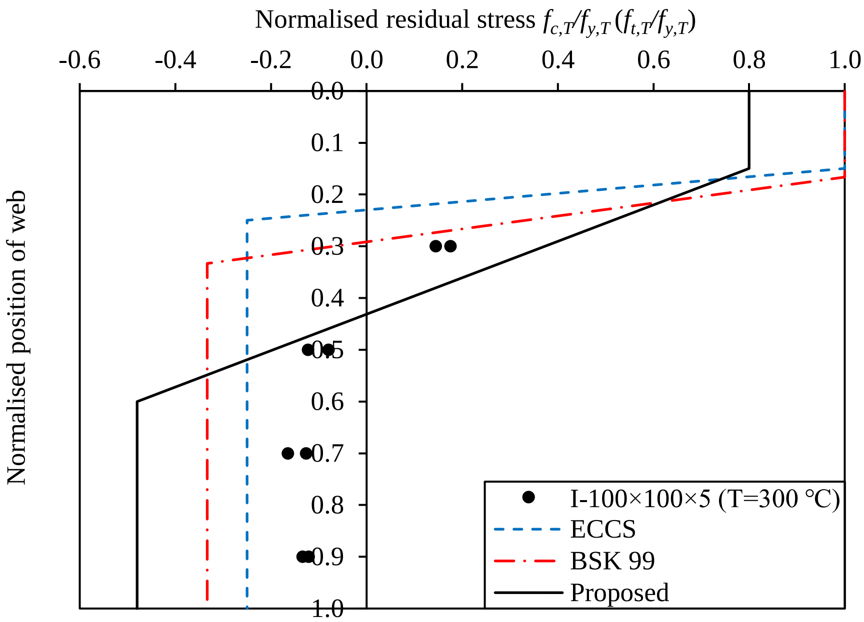

(b) Web (T=300 °C)

Fig. 17. Comparisons between measured residual stresses in S690 high strength steel welded I-section after exposure to an elevated temperature of 300 °C and predictive models.

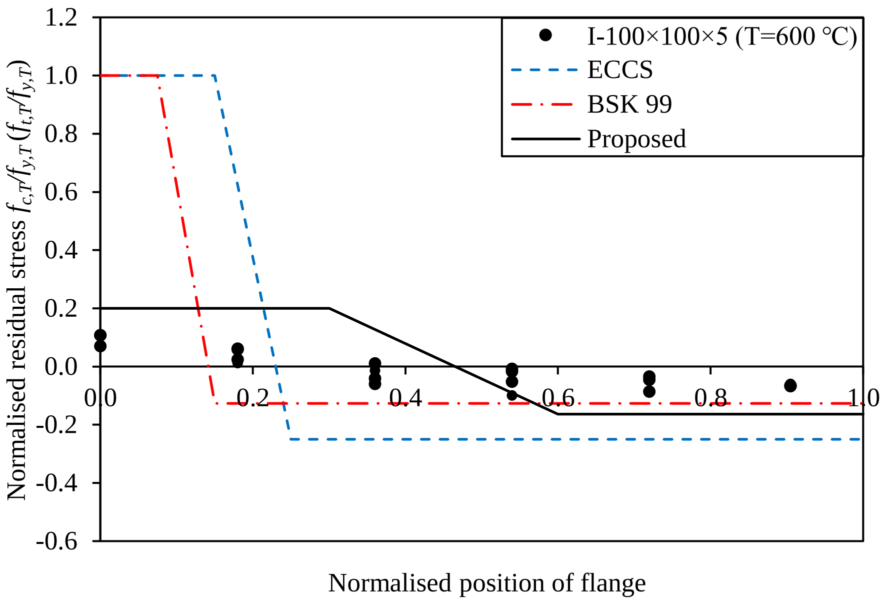

(a) Flange (T=600 °C)

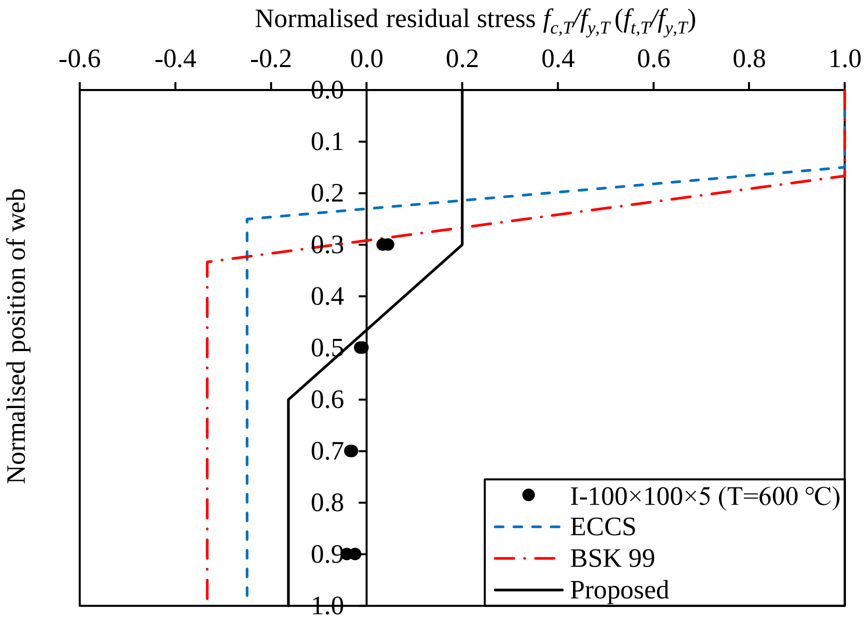

(b) Web (T=600 °C)

Fig. 18. Comparisons between measured residual stresses in S690 high strength steel welded I-section after exposure to an elevated temperature of 600 °C and predictive models.

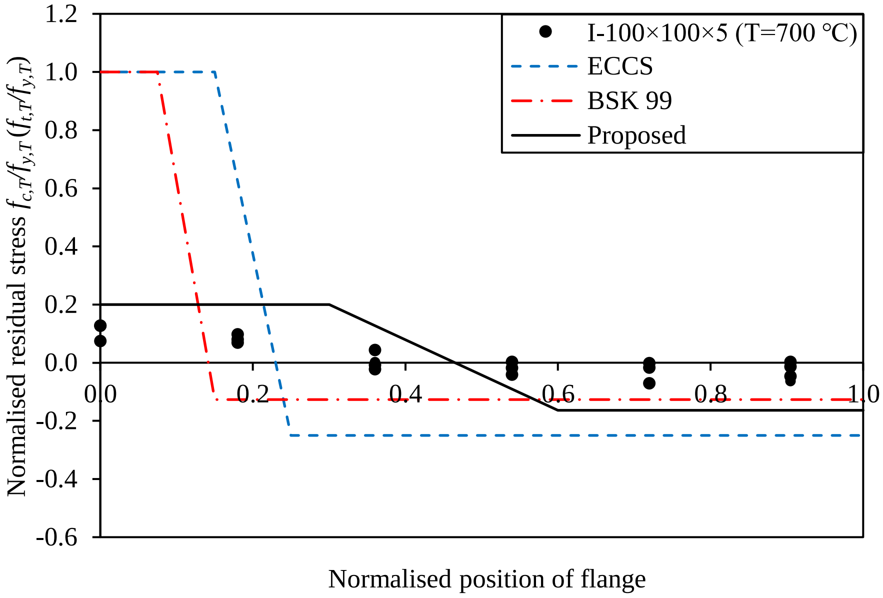

(a) Flange (T=700 °C)

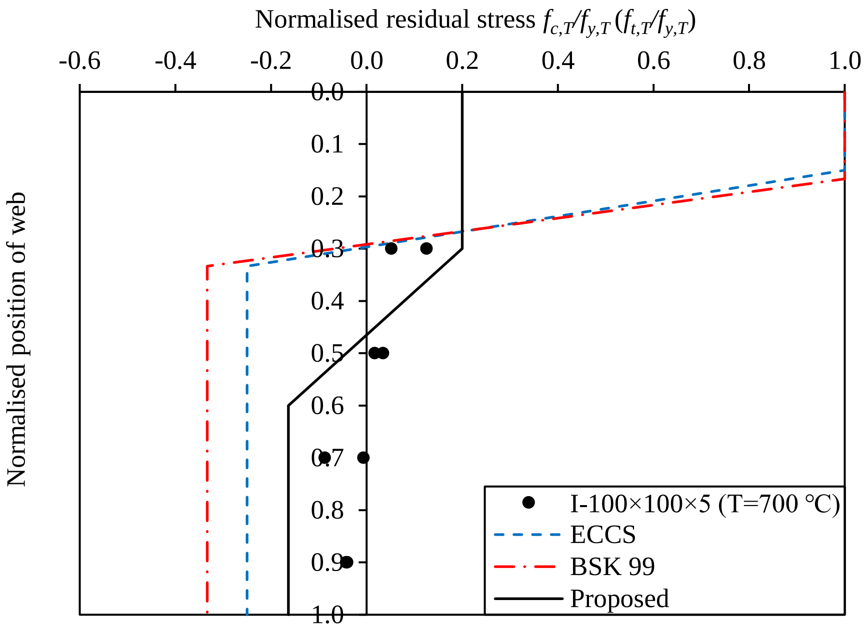

(b) Web (T=700 °C)

Fig. 19. Comparisons between measured residual stresses in S690 high strength steel welded I-section after exposure to an elevated temperature of 700 °C and predictive models.

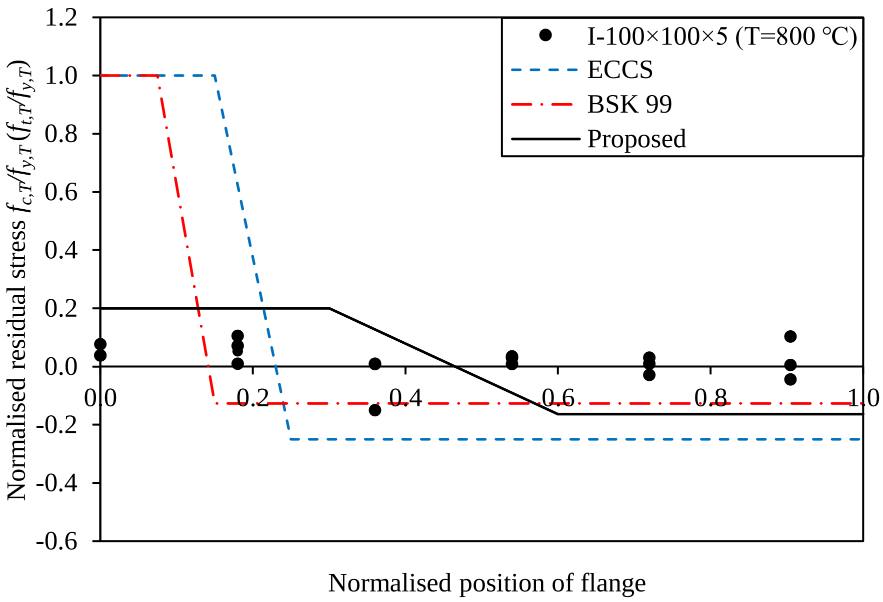

(a) Flange (T=800 °C)

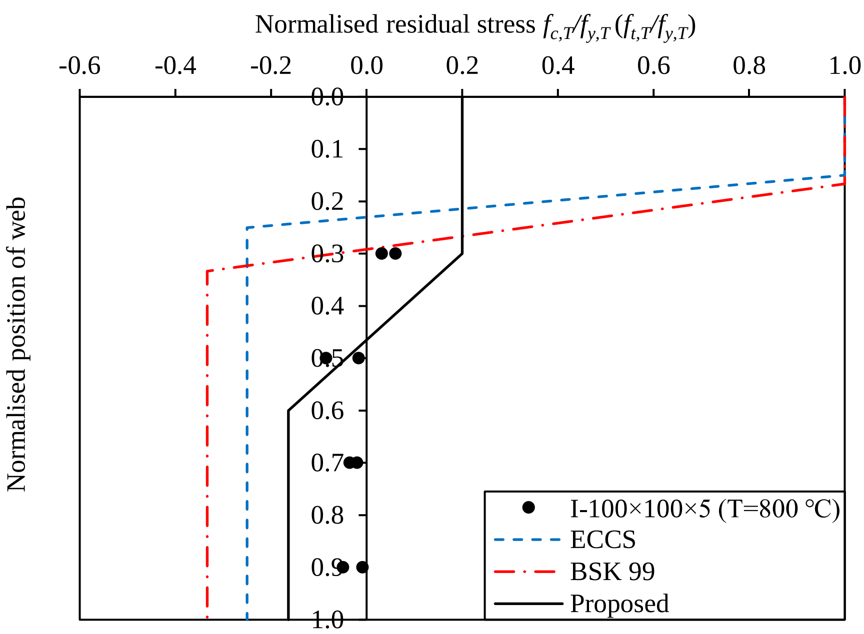

(b) Web (T=800 °C)

Fig. 20. Comparisons between measured residual stresses in S690 high strength steel welded I-section after exposure to an elevated temperature of 800 °C and predictive models.

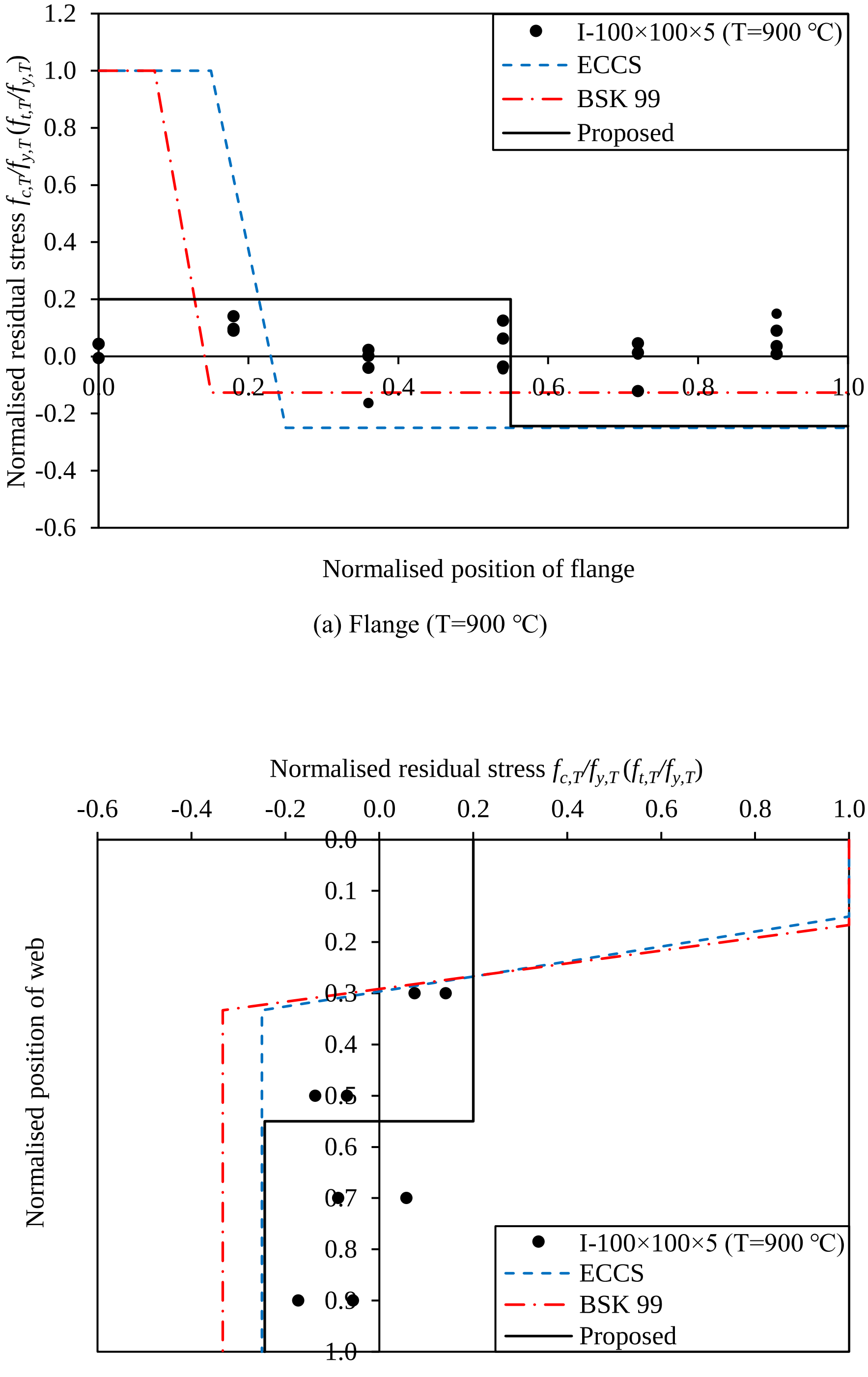

(b) Web (T=900 °C)

Fig. 21. Comparisons between measured residual stresses in S690 high strength steel welded I-section after exposure to an elevated temperature of 900 °C and predictive models.

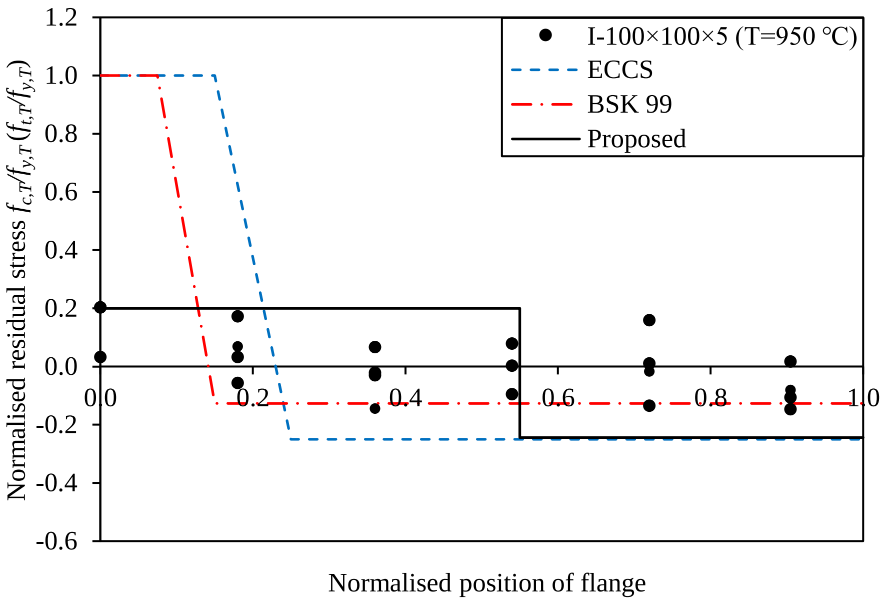

(a) Flange (T=950 °C)

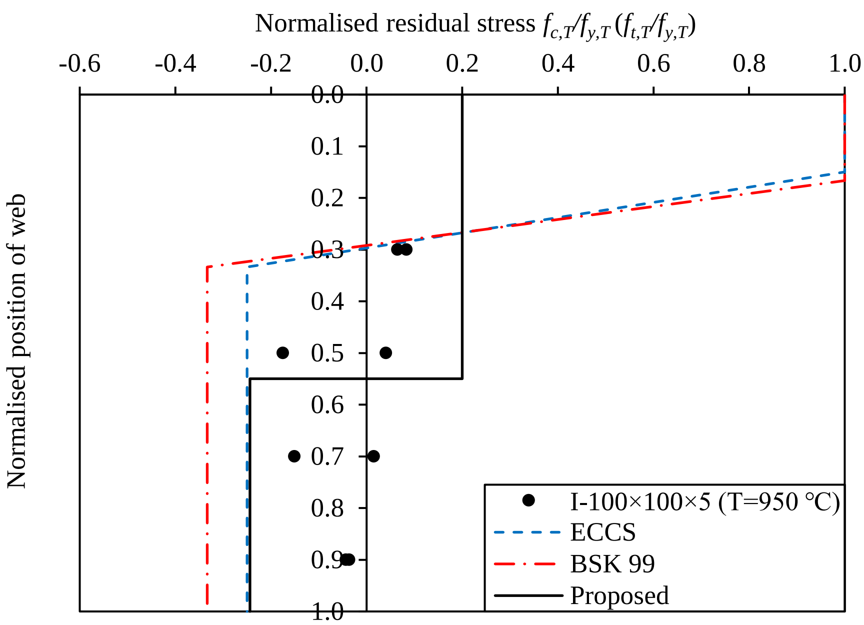

(b) Web (T=950 °C)

Fig. 22. Comparisons between measured residual stresses in S690 high strength steel welded I-section after exposure to an elevated temperature of 950 °C and predictive models.

Table 1

Summary of key material properties from S690 high strength steel longitudinal and transverse coupons.

(a) At room temperature.

Direction	Temperature (°C)	E (MPa)	f_y (MPa)	f_u (MPa)
Longitudinal	30	205369	716	794
Transverse	30	217682	866	911

(b) After exposure to elevated temperatures.

Direction	Temperature (°C)	E_T (MPa)	$f_{y,T}$ (MPa)	$f_{u,T}$ (MPa)
Longitudinal	300	204009	765	816
	600	201964	743	800
	700	195191	666	741
	800	203923	436	502
	900	190717	336	411
	950	188273	325	376
Transverse	300	217682	866	911
	600	221454	835	897
	700	221687	748	818
	800	220302	436	502
	900	202866	353	495
	950	192476	333	394

Table 2

Normalised measured peak tensile and compressive membrane residual stresses of S690 high strength steel welded I-sections at room temperature and after exposure to elevated temperatures.

Temperature (°C)	Peak tensile residual stresses ($f_{t,T}/f_{y,T}$ or f_t/f_y)		Peak compressive residual stresses ($f_{c,T}/f_{y,T}$ or f_c/f_y)	
	Flange	Web	Flange	Web
30	0.64	0.30	-0.32	-0.28
	0.70		-0.27	
300	0.54	0.18	-0.29	-0.16
	0.56		-0.25	
600	0.11	0.05	-0.09	-0.04
	0.07		-0.10	
700	0.13	0.13	-0.07	-0.09
	0.10		-0.06	
800	0.07	0.06	-0.15	-0.08
	0.11		-0.01	
900	0.14	0.14	-0.12	-0.17
	0.15		-0.16	
950	0.20	0.08	-0.15	-0.18
	0.17		-0.14	

Table 3

Post-fire retention factors for key material properties.

Direction	Temperature (°C)	E_T/E	$f_{y,T}/f_y$	$f_{u,T}/f_u$
Longitudinal	30	1.00	1.00	1.00
	300	0.99	1.07	1.03
	600	0.98	1.04	1.01
	700	0.95	0.93	0.93
	800	0.99	0.61	0.63
	900	0.93	0.47	0.52
	950	0.92	0.45	0.47
Transverse	30	1.00	1.00	1.00
	300	1.02	1.15	1.16
	600	1.03	1.11	1.14
	700	1.03	1.00	1.04
	800	1.03	0.58	0.64
	900	0.95	0.47	0.63
	950	0.90	0.44	0.50

Table 4

Membrane residual stress predictive models for welded I-sections.

Preditive model	Peak tensile residual stress	Peak compressive residual stress	a	b	c	d
ECCS [28]	1.0 f_y	-0.25 f_y	$0.05b_f$	$0.15b_f$	$0.075h_w$	$0.05\ h_w$
BSK 99 [29]	1.0 f_y	From equilibrium	$0.75t_f$	$1.5t_f$	$1.5t_w$	$1.5\ t_w$
Sun et al. [3]	0.8 f_y	From equilibrium	$0.225b_f$	$0.15b_f$	$0.075h_w$	$0.225h_w$

Note: b_f and h_w are respectively the flange width and clear distance between the flanges; t_f and t_w are the flange thickness and web thickness, respectively.

Table 5

Proposed membrane residual stress predictive model for S690 high strength steel welded I-sections after exposure to various levels of elevated temperatures.

Temperature (°C)	Peak tensile residual stress	Peak compressive residual stress	a	b	c	d
T< 500 °C	0.8 $f_{y,T}$	From equilibrium	$0.225b_f$	$0.15b_f$	$0.075h_w$	$0.225h_w$
500 °C ≤ T < 800 °C	0.2 $f_{y,T}$	From equilibrium	$0.15b_f$	$0.3b_f$	$0.15h_w$	$0.15h_w$
800 °C ≤ T ≤ 950 °C	0.2 $f_{y,T}$	From equilibrium	0	$0.55b_f$	$0.275h_w$	0